https://doi.org/10.20965/jdr.2018.p0193

Paper:

3-D Gravity Basement Structure Around Mashiki, Kumamoto, Japan

Shun Araki[1,*], Tatsuya Noguchi[2], Masao Komazawa[3], Shoya Arimura[2], Mitsuhiro Tamura[2,*], Kei Nakayama[2,*], Hitoshi Morikawa[1,†], Takashi Miyamoto[4], Kahori Iiyama[1], Yoshiya Hata[5], Masayuki Yoshimi[6], Takao Kagawa[2], and Hiroyuki Goto[7]

[1]Department of Civil and Environmental Engineering, Tokyo Institute of Technology
4259-G3-7, Nagatsuta, Midori-ku, Yokohama 226-8502, Japan
[†]Corresponding author, E-mail: morikawa.h.aa@m.titech.ac.jp
[2]Tottori University, Tottori, Japan
[3]Oyo Corporation, Tsukuba, Japan
[4]Yamanashi University, Yamanashi, Japan
[5]Osaka University, Osaka, Japan
[6]Geological Survey of Japan/AIST, Tsukuba, Japan
[7]Kyoto University, Kyoto, Japan
[*]Former student, current affiliation has been changed
[Received August 3, 2017; accepted December 4, 2017]

Gravity survey has been carried out around central part of Mashiki, Kumamoto, Japan, where was severely damaged by 2016 Kumamoto earthquake. Dense observations were performed at more than 450 sites around the central part of Mashiki. The observation sites satisfy enough density to discuss density structure shallower than 500-meter depth around the target area. After applying some corrections to the observed data, Bouguer anomaly is obtained and three dimensional model of gravity basement is estimated. As a result, a graben runs parallel to the Akitsukawa River and some isolated small basins are found inside of the graben. The central part of Mashiki is located immediately above of the one of such the small basins. We also analyze focusing and defocusing effects of ray of seismic wave under very simple assumptions and it is found that the central part of Mashiki locates close to a focusing area.

Keywords: gravity survey, 2016 Kumamoto earthquake, gravity basement, ray tracing, focusing and defocusing

1. Introduction

The 2016 Kumamoto earthquake of April, 2016 brought serious damage to Kumamoto area, Japan. Especially, JMA intensity of 7 were observed twice by Mw6.2 large earthquake of April 14, in which we call this foreshock hereafter, and Mw7.0 main shock of April 16. These sequential two earthquakes caused serious damage of wooden structures in Mashiki, Kumamoto (e.g., Yamada et al. [1], and Bai et al. [2]).

To discuss the structural damage, many researchers carried out various surveys to identify the ground structures for estimation of ground motions. For example, Hata et al. [3, 4] performed dense microtremor survey around central part of Mashiki. Target frequency range for many of microtremor survey is higher than 1 Hz, thus it is suitable to estimate very shallow velocity structure of ground. Many borehole information is available for shallow ground around Mashiki area. These information plays very important roles to discuss the local site effects of ground motions at a specific site.

On the other hand, there are few information on seismic bedrock, which corresponds to layer of hard rock and is called bedrock or basement for simplicity hereafter, not to engineering basement. Many of hamlets of Mashiki area locate on plain field around Akitsukawa and Kiyamakawa River and are surrounded by hilly or mountainous areas. Information on bedrock configuration under such the hamlets are still not enough to discuss ground motions over a regional scale.

Generally speaking, there are significant contrast of density at the boundary between sediments and bedrock. Thus, gravity survey is a useful technique to estimate bedrock configuration and various applications are available (e.g., Akamatsu et al. [5], Komazawa et al. [6], and Goto et al. [7]).

We carried out gravity survey around central part of Mashiki, Kumamoto, Japan to model a three dimensional configuration of bedrock and preliminary discussion on the earthquake ground motions.

2. Observations and Results

2.1. Gravity Survey and Bouguer Anomaly

We carried out gravity survey around central part of Mashiki, Kumamoto, Japan, where is severely damaged by 2016 Kumamoto earthquake. The observations were performed from November 28 to December 2, 2016.

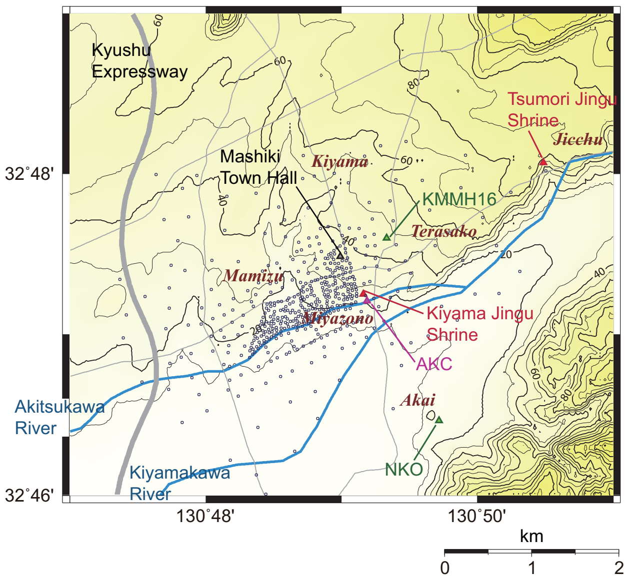

Fig. 1. Observation sites and terrain map around central part of Mashiki, Kumamoto, Japan. Blue dots are observation sites for gravity, blue solid lines are rivers, thick gray line is expressway, and thin gray lines are roads. Contour interval is 10 m for elevation. Italic letters are names of hamlets and sans-serif letters are names for typical sites.

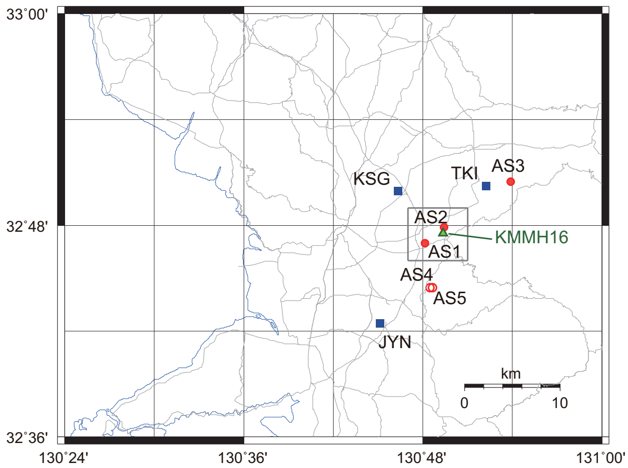

Fig. 2. Epicenters for rupture starting points of each asperity proposed by Nozu [14, 15]. Closed circles show asperities (AS1, AS2, and AS3) for main shock and open circles (AS4 and AS5) for the largest foreshock. AS4 and AS5 are almost overlapped. Blue rectangulars for GEONET stations (KSG and JYN) and reference sites for absolute gravity (TKI and KSG). The gray rectangular corresponds with the area shown in **Fig. 1**.

We applied three G-type gravimeters (G911, G1034, and G1047) manufactured by LaCoste & Romberg and one CG-3M gravimeter (S/N 258) by Schintrex. For the observations, we set a gravity reference at a parking lot for the park by Akitsukawa River, where we call this site AKC hereafter, and AKC is shown as a closed triangle in **Fig. 1**.

To minimize the error attributed to the drift nonlinearity, we measured gravity values at the AKC station three times a day: as beginning and end of the observation, and around noon.

We set observation sites more than 300 sites around the central part of Mashiki with about 50-meter intervals, where is most severely damaged area. And, more than 150 sites surround the central part with 250- to 500-meter intervals. The observation sites are shown as small dots in **Fig. 1**. The total number of sites are 463 and sites are distributed enough to discuss density structure shallower than 500-meter depth around central part of Mashiki.

The positions of sites are determined through rapid static survey, which use network RTK (real time kinematic) of a technique for GPS (global positioning system) survey, and differential survey for post processing, which refers to data of GEONET (GNSS earth observation network) system [8] provided from GSI (Geospatial Information Authority of Japan). For the latter analysis, we refer two sites of GEONET as references, that is, Kumamoto (ID: 950465, called KSG hereafter) and Jyonan (ID: 021071, called JYN), where these sites are shown in **Fig. 2**. The accuracies of the site position determination are sub-centimeter in vertical and enough for the analysis of gravity data.

The absolute value of gravity at AKC is determined from the value at KSG. The gravity values were changed

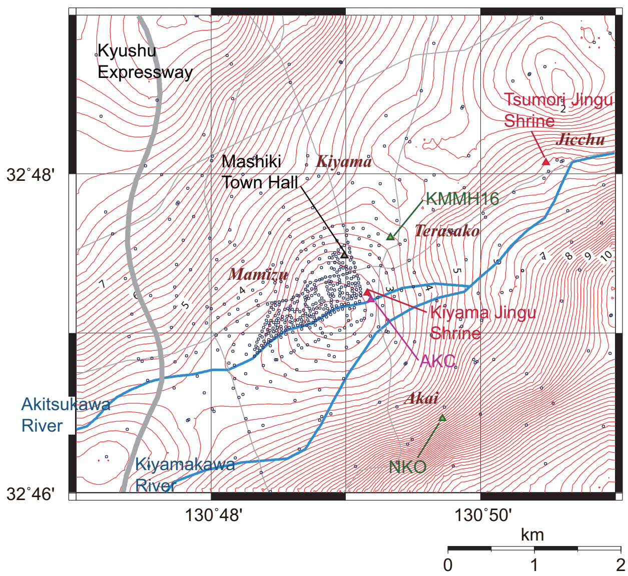

Fig. 3. Bouguer anomaly map with assumed density 2400 kg/m^3. Contour interval is 0.2 mGal.

after the 2016 Kumamoto earthquake because of diastrophism, though they updated the gravity value at a reference site, where is close to Kumamoto airport and called TKI hereafter. The value at KSG was determined through the closed observations between KSG and TKI as 979553.3896 mGal. We performed closed observations between AKC and KSG on November 28 using CG-3M, and obtained the difference of gravity values between these two sites as 6.283 mGal, thus the value at AKC is determined as 979547.107 mGal.

For the analysis of the observed gravity values, some corrections are applied, that is, instrument height, drift of gravimeter, earth tide, elevation (known as freeair cor-

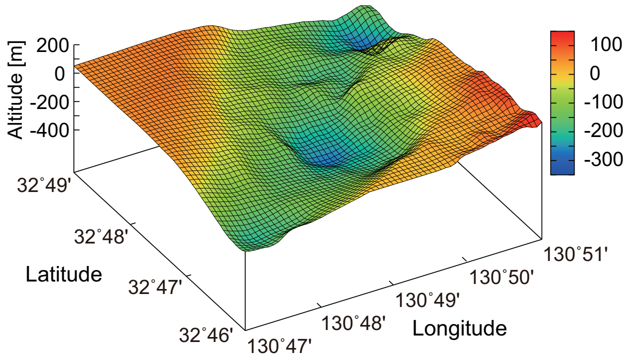

Fig. 4. Birds-eye view of gravity-basement model from south-west side. 500 kg/m^3 is applied for density contrast between basement and sediment.

rections), and terrain [9]. The assumed density is set to 2400 kg/m^3 and Bouguer anomaly is obtained as shown in **Fig. 3**. To determine the assumed density, we calculate many Bouguer anomaly maps with various values of assumed densities and choose a value which provides lowest correlation between the Bouguer anomaly and topography. The assumed density corresponds to the density of basement. For the calculation of Bouguer anomaly, we merge existent gravity data at 114 sites in the target area [10] and analyze data at 577 sites together.

2.2. Three Dimensional Model of Gravity Basement

Gravity basement is modeled to satisfy the obtained Bouguer anomaly. First, upward continuation filter [11] with band-path of 50 to 3000 meters is applied to remove gravity anomaly of regional component with a large wavelength, which corresponds to effects from very deep density structure. This means that the filtered anomaly corresponds to the density structure shallower than about 1 km depth [9]. In this depth range, the largest contrast of density must be found on a boundary between sediments and the bedrock. Thus, this suggests that the filtered anomaly reflects the bedrock configurations.

It is known from many borehole data that the sediments consist of sands and/or sand gravels and bedrock is andesite around the target area. Then, the density contrast is set 500 kg/m^3 between sediments and bedrock, whose density can be assumed as 2400 kg/m^3. The constraints of the depth to bedrock are given from borehole data at two sites: KMMH16 and NKO in **Fig. 1**. KMMH16 is an observation site for strong motion of KiK-net [12], where the borehole reaches to bedrock with 2700 m/s of shear wave velocity at 235 meters from the ground surface. A borehole at NKO also reaches to bedrock at 8.5 meters.

3D gravity basement model is shown in **Fig. 4** for birds-eye view and **Figs. 5** and **6** for contour lines with 20-meter interval. **Fig. 4** shows the view from south-west corner of the target area.

The configuration of bedrock seems to reflect the surface topography, generally. however, a graben runs parallel to the Akitsukawa River and some isolated small basins are found inside of the graben. The central part of

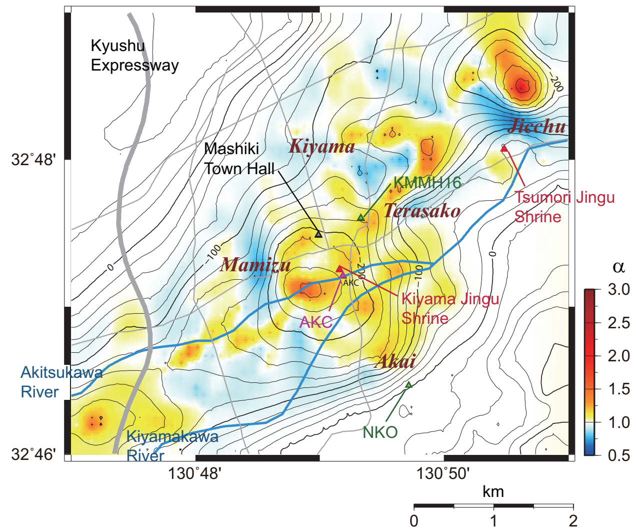

Fig. 5. Focusing and defocusing effects by bedrock configuration. Warmer color stands for much focusing effects and cooler color for defocusing. The contour lines show the altitude of boundary between sediments and bedrock with 20-meter interval.

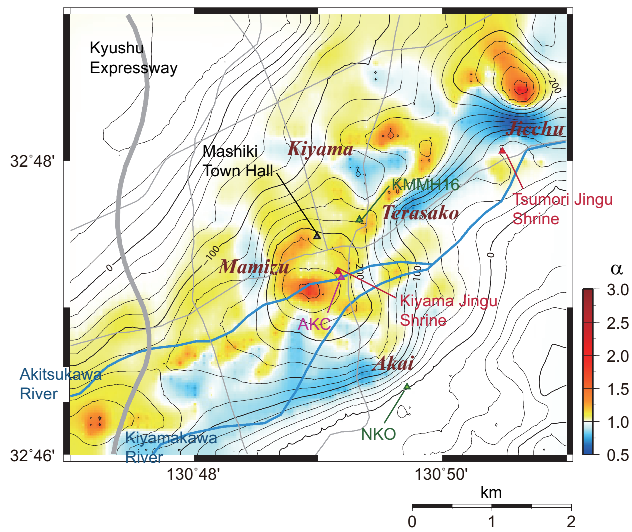

(a) Incident azimuth: 0 degree.

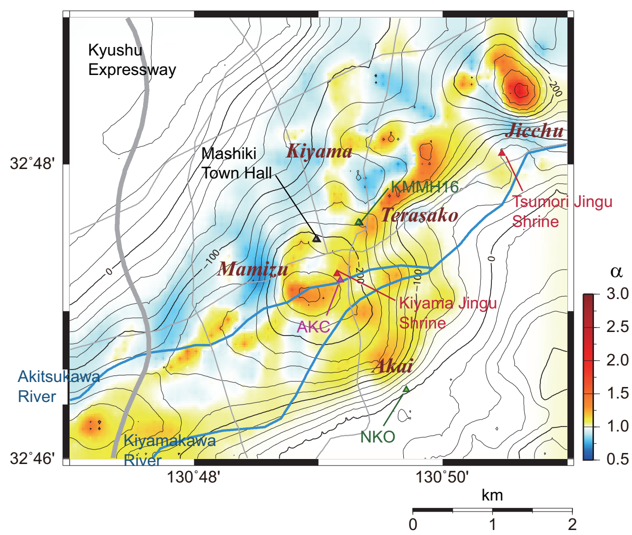

(b) Incident azimuth: 90 degree.

Fig. 6. Focusing and defocusing effects by the bedrock configuration with different incident azimuths.

Table 1. Parameters of asperities for fore- and main shocks of the 2016 Kumamoto earthquake [14, 15].

	ID of Asperity	Rupter Starting Point Longitude [deg.]	Latitude [deg.]	Depth [km]	Epicentral Distance [km]	Azimuth [deg.]	Incident angle [deg.]
Main shock	AS1	E130.802	N32.784	15.0	1.678	234.9	6.6
	AS2	E130.823	N32.797	15.0	0.839	44.9	3.3
	AS3	E130.898	N32.841	11.0	9.383	54.2	41.8
Fore-shock	AS4	E130.808	N32.742	11.0	5.588	188.3	28.0
	AS5	E130.809	N32.742	7.0	5.575	187.4	40.6

Mashiki is located immediately above of the one of such the small basins (see **Fig. 5**). The small basins are also located the north-east and south-west corner of the target area: the former is located just north of Jicchu hamlet and the latter is under the Kyushu expressway between Akitsukawa and Kiyamakawa Rivers.

3. Anomaly of Ground Motions by Seismic Wave Focusing/Defocusing Effect

The ray tracing analysis is conducted to discuss the properties of ground motion fields using the gravity basement model. Detailed numerical techniques such as the finite difference method are more suitable for the detailed discussion for ground motions than the ray tracing. The gravity basement, however, is very simple model with only two media of sediments and bedrock and properties of media are not clear, thus the simple analysis by the ray tracing will be sufficient for preliminary discussion of the ground motions.

Snell's law in 3D [13] is applied to analyze the rays of elastic waves which propagate the media obtained in the previous section. A footprint for an unit of wave packets will be expanded or condensed on the ground surface by means of the refraction at the boundary between sediments and bedrock. We introduce a parameter, α, which is a scale of seismic wave focusing and defocusing. α is defined through the ratio of the footprint area between incident wave and output wave on the surface. The focusing and defocusing arise in cases of $\alpha > 1$ and $\alpha < 1$, respectively.

For the analysis, the shear wave velocities of sediment and bedrcok are set to 760 m/s and 2700 m/s, respectively, in which these values refer the PS logging data at KMMH16 and the value for sediment is averaged value for the sediment. The waves are input parallelly to bottom of bedrock and are refracted at the boundary between sediments and bedrock. The incident direction of the wave, that is, incident angle and azimuthal angle from the north, is determined from the relative position vectors between KMMH16 and the rupture starting points for asperities of fore- and main shocks. We refer asperity models proposed by Nozu [14, 15]. Parameters of each asperity are listed in **Table 1**, and their epicenters are shown in **Fig. 2** as open circles for foreshock and closed circles for main shock.

The structural damage seems to be affected mainly by the largest asperity (AS3), and we will shows results for the distribution of focusing and defocusing effects caused by AS3 with contour lines of the gravity basement model in **Fig. 5**. In this figure, warmer and cooler color show the larger focusing and defocusing effects, respectively.

Someone may point out that the focusing area depends on the azimuth of incident waves under assumptions of parallel incident-wave packets, because the asperity locates very close to the target area. To confirm the effects of incident azimuth, we calculate focusing and defocusing effects for cases of azimuthal angle of 0 and 90 degrees. **Fig. 6** shows the results and it is observed that the comprehensive properties for distribution of forcusing areas is similar around the hamlets of Masiki area, where locate above the graven, for all the cases including **Fig. 5**. Thus, **Fig. 5** can be accepted for preliminary discussion on properties of ground motions.

4. Discussion

Three significant focused areas are found and some defocusing areas surround them as shown in **Fig. 5**. The central part of Mashiki corresponds to a one of significant focused area and there were many severely damaged structures in this area. There are very few structures and artifacts around another significant focused area of north-east part in **Fig. 5**, thus, it is difficult to find any signatures of ground motions. The Kyushu expressway runs across third focused area, where locates south-west part of the target area, and the elevated bridge of the expressway between Akitsukawa and Kiyama Rivers was severely damaged as shown in **Fig. 7(a)**.

On the other hand, many of inhabitants of Mashiki area depose that there were very few damaged structures around Jicchu hamlet, where corresponds to defocused area of north-east part. **Fig. 7(b)** shows structures in Jicchu, where less damages are found. The contrast of the structural damages suggest that the differences of the ground motions and the differences seem to reflect the properties of wave fields as shown in **Fig. 5**.

However, it is difficult to show quantitatively the differences of damage distributions. An example is introduced to demonstrate difference of damages for two similar structures located at different sites. They are Kiyama Jingu and Tsumori Jingu shrine: the former locates in the

(a) Kyushu expressway

(b) Jicchu hamlet

(c) Kiyama Jingu shrine

(d) Tsumori Jingu shrine

Fig. 7. Examples of structural damages at typical focused and defocused areas. Photos (a) and (c) are structures in focused areas and (b) and (d) are in defocused areas. Photo (a) shows an example of damaged bearings, and very few damages are found in Photo (b). Kiyama Jingu shrine was completely collapsed as shown in Photo (c), though Tsumori Jingu shrine was inclined and supported by a prop, but not collapsed as Photo (d).

focused area of central part of Mashiki, and the latter in the defocused area close to Jicchu. Their locations are shown in **Fig. 5**. Although Kiyama Jingu shrine was completely collapsed as shown in **Fig. 7(c)**, Tsumori Jingu shrine was severely damaged, but not collapsed as shown in **Fig. 7(d)**. **Fig. 7(d)** shows main structure of Tsumori Jingu shrine. Both two structures are traditional shrine structures, which have heavy roofs and less walls. The epicentral distance from AS3 to Tsumori Jingu shrine is shorter than Kiyama jingu shrine, though Tsumori Jingu shrine has survived. This suggests that the ground motions at these two sites were very different and less effective to Tsumori Jingu shrine than to Kiyama Jingu shrine.

Yamada et al. [1] investigated the damage distributions in the central part of Mashiki. The distributions are well explained by nonlinear site response and age of the buildings, because the damage is locally concentrated in approximately 250m width for north-to-south direction. Although focusing areas are not well correlated to distributions of damaged wooden buildings, the 3-D bedrock structure potentially increased the ground motion levels in the central part of Mashiki. In order to discuss the factors quantitatively, ground motion simulations based on compiling both the bedrock structure and local site response should be performed in future study.

5. Conclusions

We have carried out dense gravity survey around the central part of Mashiki, Kumamoto, Japan, where was severely damaged by the 2016 Kumamoto earthquake. A model of gravity basement is obtained to satisfy the Bouguer anomaly under the assumption of two layered medium: sediments and bedrock. It is found that a graben runs parallel to the Akitsukawa River and there are some isolated small basins inside of the graben. From the simple analysis by ray tracing technique, there are three focused areas in the target area and defocused areas surround them. In a large sense, the focused areas seem to correspond to the damaged area and defocused areas to less damaged area. However, it is very difficult to discuss the damages of individual structures from the proposed simple model.

For the future works, we have to merge any other factors relating to the ground motions such as nonlinear site response with the proposed model to discuss precisely damages of individual structures.

Acknowledgements

This work is partially supported by special research fund for collaborative research in Disaster Prevention Research Institute (DPRI), Kyoto University (28U-05 and 28U-07).

References:

[1] M. Yamada, J. Ohmura, and H. Goto, "Wooden building damage analysis in Mashiki town for the 2016 Kumamoto earthquakes on April 14 and 16," Earthquake Spectra, 2017 (in press).

[2] Y. Bai, B. Adriano, E. Mas, and S. Koshimura, "Machine learning based building damage mapping from the ALOS-2/PALSAR-2 SAR imagery: Case study of 2016 Kumamoto earthquake," Journal of Disaster Research, Vol.12, No.sp, pp. 626–655, 2017.

[3] Y. Hata, F. Minato, M. Yamauchi, Y. Okawa, Y. Ueda, S. Atoji, H. Goto, M. Yoshimi, A. Furukawa, H. Morikawa, T. Ikeda, and T. Kagawa, "Evaluation of local site effects with very high density in central Mashiki Town, Kumamoto Prefecture, Japan, Based on temporary earthquake observations and microtremor measurements, and its applications," Proceedings of the International Workshop on the 2016 Kumamoto Earthquake, Fukuoka, March 6, 2017.

[4] Y. Hata, A. Furukawa, H. Goto, M. Yoshimi, H. Morikawa, T. Ikeda, and T. Kagawa, "Investigation of tombstone condition at graveyard sites in central Mashiki Town, Kumamoto Prefecture, Japan, and its applications," Proceedings of the International Workshop on the 2016 Kumamoto Earthquake, Fukuoka, March 6, 2017.

[5] J. Akamatsu, K. Nishimura, H. Morikawa, S. Sawada, K. Onoue, H. Saito, M. Jido, T. Kagawa, K. Kamura, K. Sato, K. Furuno, and M. Komazawa, "Bedrock Structure around Faults and Its Relation to Earthquake Disaster," Earthquake Proof Design and Active Faults, (Edited by Y. Kanaori), Elsevier Science, pp. 199–216, 1997.

[6] M. Komazawa, H. Morikawa, K. Nakamura, J. Akamatsu, K. Nishimura, S. Sawada, A. Erken, and A. Onalp, "Bedrock Structure in Adapazari, Turkey – A Possible Cause of Severe Damage by the 1999 Kociaeli Earthquake –," Soil Dynamics and Earthquake Engineering, Vol.22, Nos.9–12, pp. 829–836, 2002.

[7] H. Goto, C. Takahashi, Y. Ishii, S.-Q. Ling, K. Miyakoshi, H. Morikawa, Y. Sato, S. Sawada, Y. Shingaki, Y. Suzuki, D. Takabatake, M. Joshima, "Deep subsurface structure estimateed by microtremors array observations and gravity surveys in Kashiwazaki area, Japan," Soils and Foundations, Vol.49, No.4, pp. 651–659, 2009.

[8] Web page on GEONET, http://terras.gsi.go.jp/geo_info/geonet_top.html (in Japanese) [accessed July 27, 2017]

[9] M. Komazawa, "Gravimetric analysis of Aso Volcano and its interpretation," Journal of Geodetic Society of Japan, Vol.41, pp. 17–45, 1995.

[10] Geological Survey of Japan, "Gravity CD-ROM of Japan, Ver.2," National Institute of Advanced Industrial Science and Technology (AIST), 2004.

[11] V. K. Gupta and N. Ramani, "Some aspect of regional-residual separation of gravity anomalies in a Precambrian terrain," Geophysics, Vol.45, pp. 1412–26, 1980.

[12] Strong Motion Seismograph Networks (K-NET, KiK-net), http://www.kyoshin.bosai.go.jp/ National Research Institute for Earth Science and Disaster Resilience (NIED) [accessed July. 28, 2017]

[13] K. Nisimura, J. Akamatsu, and M. Komazawa, "3D bedrock structure of Okayama plain, wset Japan, as inferred from gravity anomalies and its relation to damage distribution during the 1946, M8.0, Nankai earthquake." Proceedings of 15^{th} World Conference on Earthquake Engineering, Paper #1334, 2012.

[14] A. Nozu, "Characterized source model for foreshock (M6.5) of 2016 Kumamoto earthquake," http://www.pari.go.jp/bsh/jbn-kzo/jbn-bsi/taisin/sourcemodel/somodel_2016kumamoto_z.html, Port and Airport Research Institute (PARI) (in Japanese) [accessed July 28, 2017]

[15] A. Nozu, "Characterized source model for mains hock (M7.3) of 2016 Kumamoto earthquake," http://www.pari.go.jp/bsh/jbn-kzo/jbn-bsi/taisin/sourcemodel/somodel_2016kumamoto.html Port and Airport Research Institute (PARI) (in Japanese) [accessed July 28, 2017]

Name:
Hitoshi Morikawa

Affiliation:
Department of Civil and Environmental Engineering, Tokyo Institute of Technology

Address:
4259-G3-7, Nagatsuta, Midori-ku, Yokohama 226-8502, Japan

Brief Career:

1995 Research Associate, Kyoto University
1999 Associate Professor, Tottori University
2001 Associate Professor, Tokyo Institute of Technology
2012 Professor, ditto

Selected Publications:

- "A Method to Estimate Phase Velocities of Rayleigh Waves using Microseisms Simultaneously Observed at Two Sites," Bulletin of Seismological Society of America, Vol.94, No.3, pp. 961–976, 2004.

Academic Societies & Scientific Organizations:

- Japan Society of Civil Engineers (JSCE)
- Seismological Society of America (SSA)
- Seismological Society of Japan (SSJ)
- Society of Exploration Geophysicists of Japan (SEGJ)